An enhanced dynamic model for the actuator/amplifier pair in AMB systems

Eric H. Maslen and Carl R. Knospe
Department of Mechanical and Aerospace Engineering
University of Virginia
Charlottesville, VA 22904-4746 USA

Lei Zhu
Calnetix, Inc.
12880 Moore St.
Cerritos, CA 90703 USA

***Abstract*—Typical models for AMB actuators consist of a static linearized mapping from displacement and current to force ($f \approx -K_x x + K_i i$) and are augmented with actuator dynamics (bandwidth and gain) which act to correlate a command signal V_c to resulting current: $I(s) = G_a(s)V_c(s)$. In the present work, we show that this model misses a number of potentially important features, most notably the effect of amplifier bandwidth limitations on the term mapping displacement to force (K_x) and the related influence of journal motion induced back-EMF. In addition, we show how actuator eddy currents interact with the amplifier dynamics and how to model the resulting composite system.**

I. Introduction

Since the beginning of published literature on active magnetic bearings, the standard model for the actuator has relied on a static linearized mapping from displacement and current to force ($f \approx -K_x x + K_i i$) [1]. Later developments included amplifier dynamics in order to achieve higher fidelity. These dynamics were applied in simple way to the existing model: it was assumed that the mapping from amplifier command signal to actual current is characterized by the SISO transfer function $I(s) = G_a(s)V_c(s)$ so that $F(s) = G_a(s)K_i V_c(s) - K_x X(s)$ [2], [3].

In the present work, we show that this model misses a number of potentially important features, most notably the effect of amplifier bandwidth limitations on the term mapping displacement to force (K_x) and the related influence of journal motion induced back-EMF. In addition, we show how actuator eddy currents interact with the amplifier dynamics and how to model the resulting composite system.

The primary product of the paper is a reformulation so that

$$F \approx K_i G_a(s) V_c - K_x G_x(s) X$$

in which K_i and K_x are defined in the usual fashion and G_a is the transfer function of the power amplifier as measured with constant gap. $G_x(s)$ is similar to G_a except that its DC gain is 1.0. This formulation is developed for a single axis AMB and then generalized to an n−axis device.

In addition, when eddy currents are considered, this form can be extended as

$$F \approx K_i G_{a,ec}(s) V_c - K_x G_{x,ec}(s) X$$

to include the effect of finite lamination thickness. The transfer functions $G_{a,ec}$ and $G_{x,ec}$ are very similar to the non–eddy current models G_a and G_x but embed the transfer function

$$G_e = \frac{R^0}{R^0 + c\sqrt{s}}$$

The parameters R^0 and c are readily computed from actuator geometry and material properties.

Several examples are presented to illustrate the differences in predicted behavior between the static linearized model and this newer model, both with and without eddy current effects. In particular, we demonstrate that very stiff suspensions will tend to mask these differences but that soft suspensions – especially those employed when the AMB is used as a test actuator – will tend to emphasized these differences, resulting in very substantial error with the simpler model.

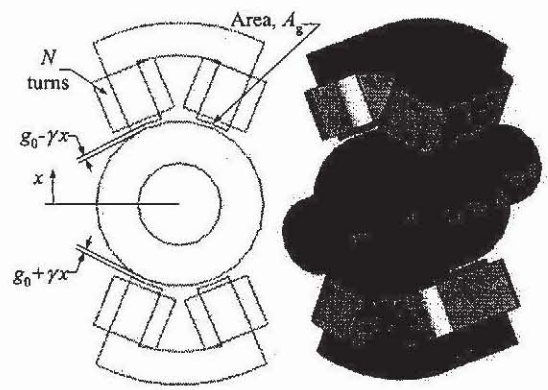

Fig. 1. Simple AMB with an opposed pair of stator quadrants.

II. Dynamics without eddy currents

Consider a simple single axis AMB actuator with two opposed horseshoe magnets as depicted in Figure 1. Each magnet has N turns (two coils wired in series, each with $N/2$ turns), pole cross section area A_g, and has its pole inclined at an angle $\cos^{-1}\gamma$ to the vertical direction. The resistance of each series connected pair of coils is R. For such a pair of magnets,

$$F = \frac{\gamma A_g}{\mu_0}\left(B_1^2 - B_2^2\right) \quad (1)$$

and (neglecting eddy current effects)

$$B_i = \frac{\mu_0 N}{2(g_0 + (-1^i)\gamma x)} I_i \tag{2}$$

Further, the coil voltages are related to B and I through

$$V_i = N A_g \frac{dB_i}{dt} + I_i R \tag{3}$$

Now, assume that each of the drive amplifiers has the control law

$$V_i = G_V(s) V_{\text{ref},i} - G_I(s) R_0 I_i \tag{4}$$

in which $R_0 \approx R$ and it may reasonably be assumed that $G_V = \alpha G_I R_0$ (the constant α sets the DC transconductance gain) although either may contain some additional filtering aimed at specific closed loop performance.

Define

$$B_b \equiv (B_1 + B_2)/2 \tag{5a}$$

$$B_p \equiv (B_1 - B_2)/2 \tag{5b}$$

so that $B_1 = B_b + B_p$ and $B_2 = B_b - B_p$ and assume that B_b is held constant. Rearrange (2) as

$$I_i = \frac{2(g_0 + (-1^i)\gamma x)}{\mu_0 N} B_i \approx \frac{2g_0}{\mu_0 N} B_i + (-1^i)\frac{2\gamma B_b}{\mu_0 N} x \tag{6}$$

With this approximation, we can expand (3) as

$$V_i = N A_g \frac{dB_i}{dt} + \frac{2 g_0 R}{\mu_0 N} B_i + (-1^i)\frac{2\gamma B_b R}{\mu_0 N} x \tag{7}$$

and (4) as

$$V_i = G_V V_{\text{ref},i} - \frac{2 G_I R_0 g_0}{\mu_0 N}\left(B_i + (-1^i)\gamma B_b \frac{x}{g_0}\right) \tag{8}$$

Equating (7) and (8) produces

$$G_V V_{\text{ref},i} - \frac{2 G_I R_0 g_0}{\mu_0 N}\left(B_i + (-1^i)\gamma B_b \frac{x}{g_0}\right) = \left(N A_g s + \frac{2 g_0 R}{\mu_0 N}\right) B_i + \frac{(-1^i) 2\gamma B_b R}{\mu_0 N} x \tag{9}$$

Define

$$V_b \equiv (V_{\text{ref},1} + V_{\text{ref},2})/2$$

and add the two instances of (9) to obtain

$$B_b = \frac{\mu_0 N G_V(0)}{2 g_0 R_0 \left(G_I(0) + R/R_0\right)} V_b \tag{10}$$

in which it is assumed that B_b and V_b are constant so that $s B_b = 0$.

Further, define

$$V_c \equiv \frac{V_{\text{ref},1} - V_{\text{ref},2}}{2}$$

and subtract the $i = 2$ instance of (9) from the $i = 1$ instance to obtain

$$B_p = \frac{\mu_0 N G_V}{\mu_0 N^2 A_g s + 2 g_0 R_0 (G_I + R/R_0)} V_c + \frac{2\gamma B_b R_0 \left(G_I + R/R_0\right)}{\mu_0 N^2 A_g s + 2 g_0 R_0 (G_I + R/R_0)} x \tag{11}$$

This may be written succinctly as

$$B_p = \frac{\mu_0 N}{2 g_0} G_a(s) V_c + \frac{\gamma B_b}{2 g_0} G_x(s) x \tag{12}$$

in which

$$L_0 \equiv \frac{\mu_0 N^2 A_g}{2 g_0} \tag{13}$$

$$G_a(s) \equiv \frac{G_V(s)}{L_0 s + R_0 G_I(s) + R} \tag{14}$$

$$G_x(s) \equiv \frac{R_0 (G_I(s) + R/R_0)}{L_0 s + R_0 G_I(s) + R} \tag{15}$$

Now, changing B coordinates as prescribed by (5), (1) produces

$$F = \frac{\gamma A_g}{\mu_0}\left(B_1^2 - B_2^2\right) = \frac{4\gamma A_g B_b}{\mu_0} B_p \tag{16}$$

Substitute (12) into (16) to obtain

$$F = \frac{2\gamma A_g B_b N}{g_0}\left(G_a(s) V_c + \frac{\gamma B_b}{\mu_0 N} G_x(s) x\right) \tag{17}$$

Define the *control* current, i, as

$$i \equiv \frac{I_1 - I_2}{2}$$

so that

$$i = \frac{G_V(s)}{L_0 s + R_0 (G_I + R/R_0)} V_c - \frac{\gamma B_b N A_g s}{2 g_0 \left(L_0 s + R_0 (G_I + R/R_0)\right)} x \tag{18}$$

Noting the previous definition of G_a (14), call G_a the *closed loop amplifier transconductance* and

$$i = G_a\left(V_c - \frac{\gamma B_b N A_g}{2 g_0 G_V} s x\right) \tag{19}$$

The first term, $G_a(s) V_c$, is the term normally included in magnetic bearing models. The second term depends on the derivative of x: it represents the effect of back–EMF induced by rotor motion and is typically not included in magnetic bearing models.

For comparison to (17), solve (19) for V_c to obtain

$$V_c = \frac{1}{G_a(s)} i + \frac{\gamma B_b N A_g s}{2 g_0} G_V(s) x \tag{20}$$

and combine (20) and (17) with definitions (14) and (15) to produce (after some algebra),

$$F = \frac{2\gamma A_g B_b N}{g_0} i + \frac{4 A_g \gamma^2 B_b^2}{\mu_0 g_0} x \tag{21}$$

Obviously, (21) is just the usual Taylor's series expansion of (1) in terms of the perturbation current, $i \equiv (I_1 - I_2)/2$, and the rotor displacement, x. Thus, assuming the form

$$F = K_i i - K_x x$$

TABLE I

EXAMPLE THRUST BEARING PARAMETERS

inner radius, inner pole piece	51.69 mm
outer radius, inner pole piece	68.32 mm
inner radius, outer pole piece	90.83 mm
outer radius, outer pole piece	101.2 mm
nominal air gap, g_0	1.0 mm
bias current, I_b	7 amps
coil turns, N	145
coil resistance, R	0.232 Ω

we obtain

$$K_i \equiv \frac{2\gamma A_g B_b N}{g_0}$$

and

$$K_x \equiv -\frac{4A_g\gamma^2 B_b^2}{\mu_0 g_0}$$

so that (17) becomes

$$F = K_i G_a(s) V_c - K_x G_x(s) x \qquad (22)$$

What is important about (22) is that, including journal motion induced back–EMF terms as in (19) and amplifier dynamics as in (4) modifies both the actuator gain term (coefficient of i in (21)) *and* the open–loop stiffness term (coefficient of x in (21)) imposing bandwidth limits to *both* terms. Further, by making G_V and G_I different, it becomes possible to maintain a high bandwidth product $K_i G_a$ while reducing the bandwidth of $K_x G_x$ substantially: this is the essential approach in *flux feedback* amplifiers. The penalty is that G_a becomes sensitive at lower frequencies to R, which can vary substantially with temperature.

A. Example: thrust bearing

To examine the effect of this dynamic limiting of K_x, consider a thrust bearing with the dimensions and parameters indicated in Table I. The amplifier transfer function $G_I = \frac{206s+578}{0.232s}$ while $G_V = 1.5\frac{206s+578}{s}$ to give a DC transconductance of 1.5 amps/volt. Because G_I is so large (a proportional gain of 887), the difference between G_a and G_x is essentially just a matter of gain, as indicated in Figure 2.

Clearly, the bandwidth of the K_x effect is the same as that of the K_i effect. This connection arises because the G_I and G_V differ only by a constant ratio. To get a notion of when this dynamic is important, consider (19). If the bus voltage driving the amplifier is 160 volts, then we begin to be concerned about amplifier saturation when the back–emf term approaches this value. That is, when

$$\left|\frac{\gamma B_b N A_g}{2g_0 G_V} s x\right| \approx 160$$

or, more conveniently, when

$$\left|\frac{x}{g_0}\right| \approx \left|\frac{320 G_V}{\gamma B_b N A_g s}\right|$$

Since $x < g_0$, we are interested in frequencies where the term to the right is less than 1.0: at lower frequencies, the voltage problem cannot arise because the motions cannot be large enough. For the present case, the frequency beyond which this condition may be met is readily found to be 52 kHz. It is very unlikely that this thrust bearing will move with an amplitude of ± 1.0 mm at a frequency as high as 52 kHz!

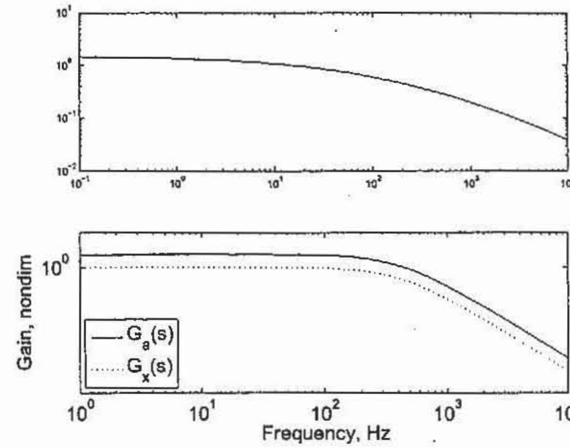

Fig. 2. Gain plots of $G_a(s)$ and $G_x(s)$ for the thrust example without eddy currents.

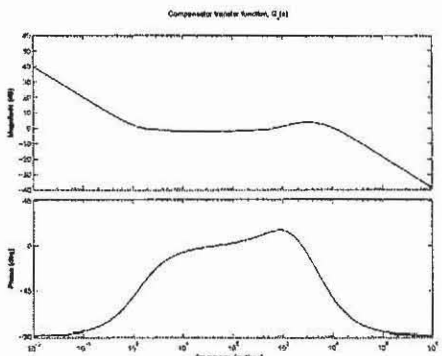

Fig. 3. Thrust bearing compensator Bode plot.

To examine the implications for stability, assume that the thrust bearing must control a mass of 34 kG and measures this mass with a sensor with sensitivity of 15000 volts/m. A PID controller is introduced with the transfer function

$$G_c(s) = \frac{0.00096s^2 + 0.8s + 1}{8\times 10^{-8}s^3 + 0.00064s^2 + s}$$

whose Bode plot is provided in Figure 3. With this compensator, the plant including bandwidth limiting on the K_x term is stable with eigenvalues of -5500, -3800, -2493, -1062, $-44.1 \pm 719j$, and -2.05. If the same system is modeled without bandwidth limiting on the K_x term, the resulting closed loop system is not stable and has eigenvalues of -5543, -3846, -1126, 7.35 ± 696, -2.05.

Not surprisingly, bandwidth limiting the K_x term improves the stability of the system (hence the interest in flux feedback). For systems of this sort with relatively minor influence of this bandwidth limitation, it is probably conservative to ignore the effect, although it is not costly to include it.

III. Dynamics with Eddy Currents

To consider the effect of eddy currents, we appeal to the developments in [4]. In that work, it is shown that the relationship between coil current, gap flux, and gap variation is closely approximated by

$$\phi_p(s) = \frac{N}{\mathcal{R}^0 + c\sqrt{s}} I_p(s) - \frac{\partial g}{\partial x_p} \frac{2NI_b}{\mu_0 A_g \mathcal{R}^0} \frac{1}{\mathcal{R}^0 + c\sqrt{s}} X_p(s) \tag{23}$$

in which the subscript p indicates small perturbations about an equilibrium point. The coefficient c characterizes the eddy current production in the material: large c implies high bulk conductivity. The constant nominal circuit reluctance, $\mathcal{R}^0$, is defined for our purposes as

$$\mathcal{R}^0 \equiv \frac{2g_0}{\mu_0 A_g}$$

Thus, we may rearrange (23) as

$$B_i(s) = \frac{\mu_0 N I_b}{2g_0} \frac{1}{1 + c'\sqrt{s}} \left(\frac{I_i(s)}{I_b} - (-1)^i \gamma \frac{x(s)}{g_0} \right) \tag{24}$$

in which

$$c' \equiv \frac{\mu_0 A_g}{2g_0} c$$

Following the previous development but using this modified relationship between flux, current, and displacement, it is fairly direct to obtain the modified model

$$\begin{aligned} F &= K_i G_a(s;c')V_c - K_x G_x(s,c')x & (25) \\ G_a(s;c') &\equiv \frac{G_V}{L_0 s + (1 + c'\sqrt{s})(G_I R_0 + R)} & (26) \\ G_x(s;c') &\equiv \frac{(R + G_I R_0)}{L_0 s + (1 + c'\sqrt{s})(G_I R_0 + R)} & (27) \end{aligned}$$

A. Example

To illustrate the alteration this produces, consider the previous example thrust bearing. Here, the parameter c has been estimated from experimental work as $c \approx 0.015 \mathrm{A/Tm^2\sqrt{sec}}$. For comparison, the gain and phase of the transfer functions $G_a(s)$ and $G_a(s;c')$ are plotted in Figure 4. The functions $G_x(s)$ and $G_x(s;c')$ have the same character.

It is particularly interesting to note that both the non–eddy current model and that including the eddy currents reach a phase of -45^o at the same frequency (about 400 Hz).

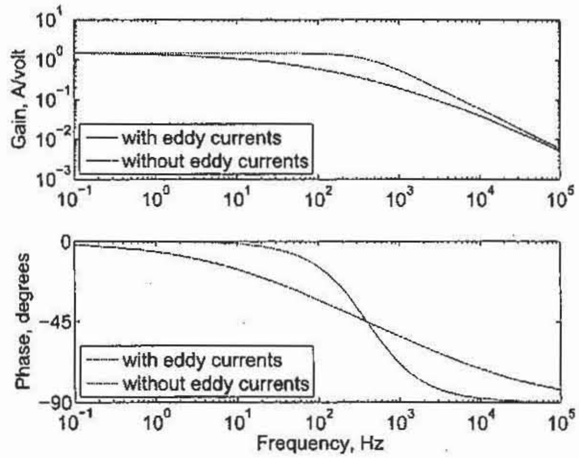

Fig. 4. Bode diagrams of $G_a(s)$ (no eddy currents in the model) and $G_a(s, c')$ (includes eddy currents in the model).

IV. Extension to Generalized Actuators

For a general actuator, the relationship between the actuator gap flux density distribution $\underline{B}$ and force in any given direction $\hat{y}$ is [5]

$$F_y \equiv \underline{F} \cdot \hat{y} = \frac{1}{2\mu_0} \underline{B}^\top \mathcal{A}_y \underline{B} \tag{28}$$

in which

$$\mathcal{A}_y = \mathrm{diag}[\mathcal{A}_{y,i}]$$

and

$$\mathcal{A}_{y,i} = -\underline{A}_i \cdot \hat{y}$$

that is, the diagonal elements of $\mathcal{A}_y$ are the dot product of the outward normal to each pole's area and the direction $\hat{y}$ in which the force is measured. The magnitude of $\mathcal{A}_i$ is the gap area of the i^{th} pole face.

The vector of gap fluxes $\underline{B}$ is related to the coil currents $\underline{I}$ and rotor position $\underline{x}$ by

$$\mathcal{R}(\underline{x})\underline{B} = \mathcal{N}\underline{I} \tag{29}$$

By Faraday's and Ohm's laws, the voltages across the coils are

$$\underline{V} = \mathcal{N}\frac{d}{dt}\underline{B} + R\underline{I}$$

Differentiating (29) produces

$$\mathcal{R}(\underline{x})\frac{d}{dt}\underline{B} + \sum_{i=1}^{n} \frac{d\mathcal{R}}{\underline{x}_i} \underline{B} \frac{d\underline{x}_i}{dt} = \mathcal{N}\frac{d\underline{I}}{dt} \tag{30}$$

so that, assuming $\mathcal{R}^{-1}$ exists,

$$\frac{d}{dt}\underline{B} = \mathcal{R}^{-1}\left(\mathcal{N}\frac{d\underline{I}}{dt} - \sum_{i=1}^{n} \frac{d\mathcal{R}}{\underline{x}_i} \underline{B} \frac{d\underline{x}_i}{dt} \right) \tag{31}$$

and, finally,

$$\underline{V} = \mathcal{N}\mathcal{R}^{-1}\left(\mathcal{N}\frac{d\underline{I}}{dt} - \sum_{i=1}^{n} \frac{d\mathcal{R}}{\underline{x}_i} \underline{B} \frac{d\underline{x}_i}{dt} \right) + R\underline{I} \tag{32}$$

Typically, the coils are wound in series sets so that

$$\underline{V}_s = \mathcal{C}^\top \underline{V}$$

which dictates that the coil currents in the coils of these series sets are given by

$$\underline{I} = \mathcal{C}\underline{I}_s$$

so that the coil voltages for the series sets are governed by

$$\underline{V}_s = \mathcal{C}^\top \mathcal{N}\mathcal{R}^{-1}\left(\mathcal{N}\mathcal{C}\frac{d\underline{I}_s}{dt} - \sum_{i=1}^{n}\frac{d\mathcal{R}}{\underline{x}_i}\underline{B}\frac{d\underline{x}_i}{dt}\right) + \mathcal{C}^\top R\mathcal{C}\underline{I}_s \tag{33}$$

Define

$$L_s \equiv \mathcal{C}^\top \mathcal{N}\mathcal{R}^{-1}\mathcal{N}\mathcal{C}\Big|_{\underline{x}=\underline{x}_0}$$

$$Q = [\underline{Q}_i] \quad : \quad \underline{Q}_i \equiv \mathcal{R}^{-1}\frac{d\mathcal{R}}{d\underline{x}_i}\underline{B}\Big|_{\underline{x}=\underline{x}_0,\underline{B}=\underline{B}_0}$$

and

$$R_s \equiv \mathcal{C}^\top R\mathcal{C}$$

to obtain the simpler statement

$$\underline{V}_s = L_s\frac{d\underline{I}_s}{dt} - \mathcal{C}^\top \mathcal{N}Q\frac{d\underline{x}}{dt} + R_s\underline{I}_s \tag{34}$$

Now, assume a control law for the amplifier array:

$$\underline{V}_s = G_V(s)\underline{V}_c - R_{s,0}G_I(s)\underline{I}_s$$

so that

$$(L_s s + R_s + R_{s,0}G_I)\underline{I}_s = G_V\underline{V}_c + \mathcal{C}^\top \mathcal{N}Qs\underline{x}$$

or,

$$\underline{I}_s = (L_s s + R_s + R_{s,0}G_I)^{-1}\left(G_V\underline{V}_c + \mathcal{C}^\top \mathcal{N}Qs\underline{x}\right)$$

which may be written as

$$\underline{I}_s = G_a(s)\left(\underline{V}_c + G_V^{-1}\mathcal{C}^\top \mathcal{N}Qs\underline{x}\right) \tag{35}$$

in which

$$G_a(s) \equiv (L_s s + R_s + R_{s,0}G_I(s))^{-1}G_V(s)$$

Referring back to (28),

$$\begin{aligned} F_y &\approx \frac{1}{\mu_0}\underline{B}^\top \mathcal{A}_y\frac{\partial}{\partial \underline{I}_s}\underline{B}\left(\underline{I}_s - \underline{I}_{s,0}\right) \\ &\quad + \frac{1}{\mu_0}\underline{B}^\top \mathcal{A}_y\frac{\partial}{\partial \underline{x}}\underline{B}\left(\underline{x} - \underline{x}_0\right) \qquad (36) \\ &= \frac{1}{\mu_0}\underline{B}^\top \mathcal{A}_y\left(\mathcal{R}^{-1}\mathcal{N}\mathcal{C}\left(\underline{I}_s - \underline{I}_{s,0}\right) - Q\left(\underline{x} - \underline{x}_0\right)\right) \end{aligned}$$

Define

$$K_{i,y} \equiv \frac{1}{\mu_0}\underline{B}^\top \mathcal{A}_y\mathcal{R}^{-1}\mathcal{N}\mathcal{C} \quad \text{and} \quad K_{x,y} \equiv \frac{1}{\mu_0}\underline{B}^\top \mathcal{A}_y Q$$

so that

$$F_y \approx K_{i,y}\left(\underline{I}_s - \underline{I}_{s,0}\right) - K_{x,y}\left(\underline{x} - \underline{x}_0\right) \tag{37}$$

As previously, substitute (35) into (37) to obtain

$$\boxed{F_y \approx K_{i,y}G_a(s)\underline{V}_{c,p} + \left(K_{i,y}G_V^{-1}\mathcal{C}^\top \mathcal{N}Qs - K_{x,y}\right)\underline{x}_p} \tag{38}$$

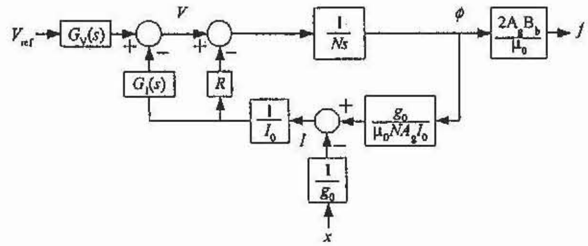

Fig. 5. Schematic view of the actuator/amplifier/rotor interaction. Eddy currents are not indicated

V. System observations

One useful feature of this expanded view of the dynamics of the amplifier/actuator interaction is that it makes accessible some important signals. An obvious way to model the interaction is indicated in Figure 5. With this structure, signals like coil voltage (V) and perturbation flux (ϕ) become accessible as part of the model signal set. These signals can be very useful in evaluating system performance – where voltage should be compared to amplifier supply voltage and flux (plus bias flux) should be compared to saturation levels for the actuator. This is especially valuable when synthesizing controllers using methods like $\mathcal{H}_\infty$ or μ where cost functions should explicitly weight these signals.

VI. Conclusions

The dynamic interaction of the actuator, amplifier, and rotor motion of an active magnetic bearing were reformulated to properly account for the effects of finite amplifier bandwidth on not only the actuator's effective gain but also its negative stiffness. Although the effect for practical bearings is not strong, the formulation does offer higher fidelity than existing models and has advantages in terms of available signals when used in some control synthesis frameworks. Further, the effect of eddy currents on these properties was also explored using a simple fractional derivative model which has been shown to exhibit high fidelity. Extension to generalized actuators was developed leading to a matrix formulation with a form similar to the forgoing scalar result.

References

[1] Schweitzer, G., "An active magnetic hub bearing–design and application," *Regelungstechnik,* Vol. 21, No. 1, January 1978, pp. 10-15.

[2] Fittro, Roger L., Knospe, C.R., and Stephens, L.S., "Experimental results of μ synthesis applied to point compliance minimization," Proceedings of the 5th International Symposium on Magnetic Bearings, Kanazawa, Japan, August 28-30, 1996.

[3] Maslen, E. H., and Montie, D. T., "Sliding mode control of magnetic bearings: a hardware perspective," ASME *Journal of Engineering for Gas Turbines and Power,* Vol. 123, No. 4, October 2001, pp. 878-885.

[4] L. Zhu, C.R. Knospe, and E.H. Maslen, "An Analytic Model for a Non-laminated Cylindrical Magnetic Actuator including Eddy Currents"

[5] D. T. Montie and E. H. Maslen, "Self-sensing in fault tolerant magnetic bearings," ASME *Journal of Engineering for Gas Turbines and Power,* Vol. 123, No. 4, pp. 864-870, October 2001.